Comparison of 1D and 2D Finite Difference Methods for Molten Salt Solidification Prediction in a Molten Salt/sCO₂ PCHE

Jeong Min Baek [a], Sungwook Choi [a], Jeong Ik Lee [a*]
[a] *Dept. Nuclear & Quantum Eng., KAIST, 291 Daehak-ro, Yuseong-Gu, Daejeon 34141, Republic of Korea*
[a*] *Corresponding author: jeongiklee@kaist.ac.kr*

Keywords : sCO_2 Cycle, PCHE, Coolant-Salt Solidification, 2D FDM

1. Introduction

In accordance with the International Maritime Organization (IMO) GHG Strategy, achieving carbon neutrality in the maritime industry has become an essential task [1]. To accomplish this goal, a transition from conventional fossil-fuel based propulsion systems to zero-carbon alternatives is required, and nuclear propulsion has emerged as one of the most promising options. Among these technologies, propulsion systems combining a molten salt reactor (MSR) and a supercritical carbon dioxide (sCO_2) cycle have recently received significant attention [2].

In such systems, the coolant-salt and the CO_2 of the power conversion system exchange heat through an intermediate heat exchanger (IHX). Since the coolant-salt solidifies below its melting point, a risk of solidification exists when the IHX inlet CO_2 temperature becomes sufficiently low. In this context, Baek et al. investigated the coolant-salt solidification phenomenon in the IHX under part-load operating conditions of an MSR–sCO_2 marine propulsion system [2]. The IHX considered in that study was a printed circuit heat exchanger (PCHE), and the coolant-salt solidification phenomenon in this PCHE-type IHX was evaluated using a one-dimensional finite difference method (1D FDM)-based analysis. The 1D FDM, which is widely used for conventional PCHE design and performance evaluation, simplifies complex internal flow paths into an ideal counter-flow configuration and merges all channels into a single representative flow path. This methodology offers the significant advantage of high computational efficiency.

When general fluids such as water or CO_2 are used as hot-side fluid, solidification due to phase change is not an issue, and therefore it is usually sufficient to evaluate the heat exchanger performance based on the average output temperature. However, when coolant-salt is used as the hot-side fluid, a new issue arises. Since the coolant-salt solidifies below its melting point, relying solely on the average outlet temperature is insufficient. Instead, identifying the local minimum temperature inside the channels becomes a critical issue for ensuring the thermal integrity and operability of the heat exchanger.

Actual PCHEs are manufactured by diffusion bonding plates etched with microchannels, and they inherently include manifold and header regions near the inlets and outlets to distribute and collect fluid among individual channels [3]. The 1D FDM inherently neglects these header regions and the induced cross-flow effects, and thus cannot represent the transverse local temperature gradients that develop in an actual PCHE. Consequently, due to the structural limitations of the 1D model, it is difficult to accurately predict coolant-salt solidification caused by local temperature drops.

To reflect the actual structural characteristics of PCHEs, a two-dimensional difference method (2D FDM) analysis is required. Unlike the 1D FDM, the 2D FDM discretizes the heat exchanger not only in the axial direction but also in the transverse direction. This methodology incorporates the actual geometric shapes of the headers and manifolds into the analysis, thereby explicitly calculating the flow maldistribution that occurs as the fluid is distributed into each microchannel, as well as the thermal behavior in the cross-flow regions [4]. Consequently, it can capture the varying mass flow rates and temperature profiles formed in individual channels, together with the heat transfer interactions between neighboring channels. Although the 2D FDM analysis has the disadvantage of a more complex numerical model and longer computational time than the 1D FDM analysis, it reveals the transverse non-uniform temperature distributions that are entirely omitted in the 1D FDM analysis. Therefore, to capture the phenomenon in which the local temperature inside specific channels drops below the melting point due to flow maldistribution near the headers when low-temperature CO_2 enters, and to identify the resulting localized solidification, a 2D FDM analysis is necessary.

Accordingly, this study comparatively investigates the solidification prediction results obtained from 1D and 2D FDM analyses for a molten salt/sCO_2 PCHE. First, the difference in performance prediction between the two numerical approaches is examined under the design-point condition. Then, an off-design condition is considered in which the IHX inlet CO_2 temperature becomes lower than the melting point of the coolant-salt. Through this comparison, the study clearly identifies the structural limitations of the conventional 1D FDM analysis in predicting localized coolant-salt solidification. In addition, the influence of a simplified channel blockage scenario is examined based on the 2D FDM results in order to discuss the possible thermal-hydraulic consequences after localized solidification onset. Furthermore, based on the 2D FDM analysis results, this study aims to provide practical guidelines for the design

and safe operation of actual MSR–sCO_2 systems, such as proposing a minimum IHX inlet CO_2 temperature condition and control margins to effectively prevent the localized solidification of the coolant-salt.

2. Methods and Results

2.1 Target IHX Design Condition

In this study, the geometric configuration and operating conditions of the target IHX were established based on the previous study by Baek et al. [2]. Baek et al. designed a PCHE-type IHX for a 100 MW_{th} marine MSR propulsion system, and the present study adopts this IHX as the reference design. The channel geometry and flow configuration of the reference IHX are illustrated in Figures 1 and 2, respectively. Its detailed geometric specifications are summarized in Table 1, and the design inlet conditions for the hot and cold channels are presented in Table II.

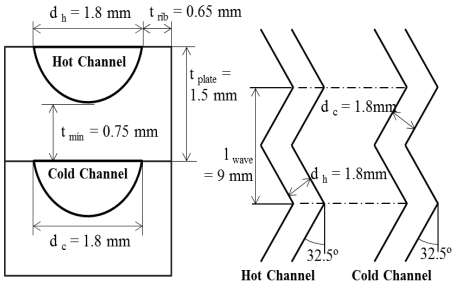

Fig. 1. Channel Geometry of Reference IHX

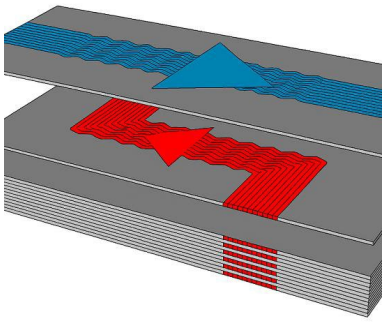

Fig. 2. Flow Configuration of Reference IHX

Table I: Geometric Specifications of the Reference IHX

Parameter	Value
Hot Side	
Channel Diameter [mm]	1.8
Channel Number	880000
Channel Length [m]	0.96
Cold Side	
Channel Diameter [mm]	1.8
Channel Number	880000
Channel Length [m]	0.96

Table II: Design Inlet Conditions of the Reference IHX

Parameter	Value
Hot Side	
Fluid	NaCl–KCl–$MgCl_2$ (30.2–22.7–47.1 mol%)
Inlet / Outlet Temperature [°C]	640 / 500
Inlet / Outlet Pressure [MPa]	1 / 0.91
Mass Flow Rate [kg/s]	649.35
Cold Side	
Fluid	CO_2
Inlet / Outlet Temperature [°C]	485.75 / 630
Inlet / Outlet Pressure [MPa]	19.7 / 19.57
Mass Flow Rate [kg/s]	558.08

2.2 Coolant-Salt

The coolant-salt selected as the working fluid for the hot side of the reference IHX is the chloride-based NaCl–KCl–$MgCl_2$. As shown in the phase diagram in Figure 3, this coolant-salt adopts the eutectic composition of 30.2–22.7–47.1 mol%, which has the lowest melting point. The melting point of this specific composition is 385°C. Therefore, in the subsequent numerical analyses, it is assumed that solidification occurs when the coolant-salt temperature at the IHX outlet or the local coolant-salt temperature inside the channels falls below this melting point. The thermophysical properties of the coolant-salt utilized in this study are summarized in Table III [5].

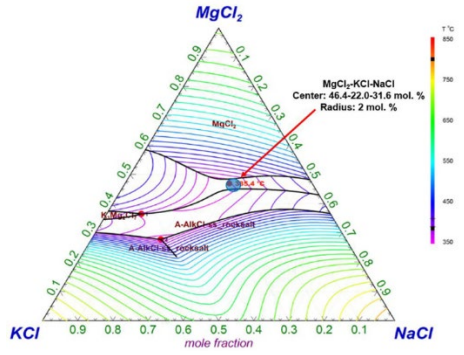

Fig. 3. Phase Diagram of NaCl–KCl–$MgCl_2$ (FactSage)

Table III: Summary of Thermophysical Properties of the NaCl–KCl–$MgCl_2$ (30.2–22.7–47.1 mol%) [5]

Property	Values or Correlations with T [°C]
Melting Point [°C]	385
Heat Capacity [J/kg · °C]	1100
Viscosity [Pa · s]	$27.728 \times 10^{-3} \times e^{-0.00364 \times T[°C]}$
Density [kg/m^3]	$1940 - 0.42 \times T[°C]$
Thermal Conductivity [W/m · °C]	$0.53 - 1.32 \times 10^{-4} \times T[°C]$

In the present study, the onset of solidification is conservatively identified based on whether the local coolant-salt temperature falls below the melting point. Accordingly, the thermophysical properties summarized in Table III are used to describe the liquid-phase behavior of the coolant-salt, while the latent heat release during solidification is not explicitly incorporated into the present numerical model. Therefore, the present analysis is intended for conservative screening of localized solidification onset rather than for fully coupled simulation of solidification growth.

2.3. KAIST-HXD for Numerical Analysis

The numerical analyses in this study were conducted using KAIST-HXD, an in-house code developed at KAIST specifically for the design and performance evaluation of PCHE-type heat exchangers. The code incorporates both 1D and 2D FDM models, enabling not only the geometric design of the heat exchanger but also performance evaluations under off-design operating conditions [4], [6]. The computational algorithms applied to the 1D and 2D FDM models are presented in Figures 4 and 5, respectively. As illustrated in the flowcharts, the 1D model discretizes the effective heat transfer region into axial nodes and sequentially updates the thermophysical properties and heat transfer rates at each node until the nodal temperatures converge. In contrast, the 2D model calculates the mass flow distribution for individual channels and explicitly divides the analysis domain into counter-flow and cross-flow regions. It then performs iterative calculations until the outlet pressure across all channels becomes uniform, thereby simulating the flow maldistribution induced by the actual structural characteristics of the heat exchanger.

Based on this computational framework, the present study first performed comparative 1D and 2D FDM analyses under the design-point inlet conditions listed in Table II in order to establish a baseline for the performance-prediction difference between the two numerical models. Table II summarizes the reference inlet conditions of the hot and cold streams used for the design-point analysis. Through this baseline comparison, the study examined the inherent discrepancy between the 1D model, which assumes an ideal counter-flow configuration, and the 2D model, which explicitly accounts for the realistic header geometry, cross-flow regions, and the resulting flow maldistribution.

Subsequently, an off-design operating condition was considered to compare the 1D and 2D FDM predictions under a condition where the cold-side inlet CO_2 temperature decreases below the melting point of the selected coolant-salt. In this study, the off-design condition was defined such that the IHX inlet CO_2 temperature was 375℃, which is 10℃ lower than the melting point of 385℃. The detailed inlet conditions adopted for this off-design analysis are summarized in Table IV. By comparing the 1D and 2D FDM predictions under the same off-design condition, the present study aims not only to identify the difference in general thermal-hydraulic performance prediction, but also to examine the discrepancy between the two models in predicting localized coolant-salt solidification.

Table IV: Off-Design Operation Conditions for the Numerical Analysis

Parameter	Value
Hot Side	
Fluid	NaCl–KCl–$MgCl_2$ (30.2–22.7–47.1 mol%)
Inlet Temperature [℃]	640
Inlet Pressure [MPa]	1
Mass Flow Rate [kg/s]	649.35
Cold Side	
Fluid	CO_2
Inlet Temperature [℃]	375
Inlet Pressure [MPa]	19.7
Mass Flow Rate [kg/s]	558.08

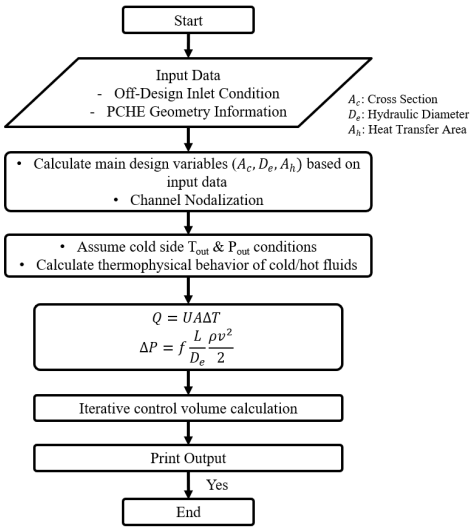

Fig. 4. Main Algorithm of the 1D FDM KAIST-HXD [6]

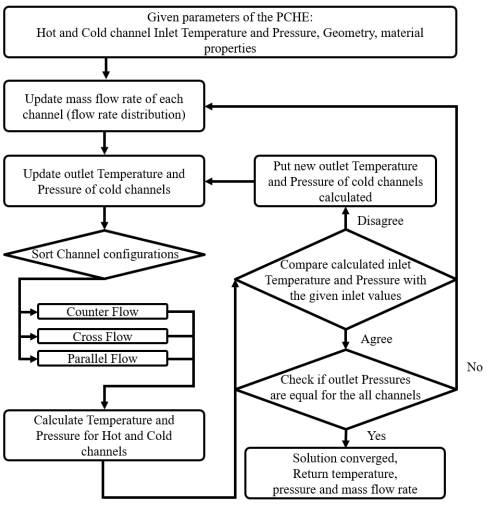

Fig. 5. Main Algorithm of the 2D FDM KAIST-HXD [4]

2.4. Results

The design-point numerical analysis results obtained from the 1D and 2D FDM KAIST-HXD are summarized in Table V. Under the design-point condition, clear differences are observed between the two numerical approaches. Compared with the 1D model, the 2D model predicts a lower heat duty, a slightly smaller temperature drop in the hot channel, a slightly smaller temperature rise in the cold channel, and significantly larger pressure drops on both the hot and cold sides. These difference arise from the fact that the 1D model assumes an ideal counter-flow configuration, whereas the 2D model explicitly accounts for the realistic header geometry, cross-flow regions, and channel-wise flow maldistribution. Therefore, the design-point comparison demonstrates that the 2D model yields these specific results for the internal flow and heat transfer behavior of the PCHE precisely because it incorporates these structural characteristics.

Table V: 1D and 2D FDM Analysis Results under the Design Conditions

	1D	2D
Hot / Cold Channel Diameter [mm]	1.8	
Length [m]	0.96	
Hot Channel Number	880000	
Cold Channel Number	880000	
Hot Inlet Temperature [℃]	640	
Hot Outlet Temperature [℃]	500.01	503.48
Cold Inlet Temperature [℃]	485.75	
Cold Outlet Temperature [℃]	630.00	629.15
Hot Pressure Drop [kPa]	85.66	196.36
Cold Pressure Drop [kPa]	129.46	240.69
Heat Duty [MW_{th}]	99.99	97.06

The off-design numerical analysis results are summarized in Table VI. Figure 6 presents the temperature profile predicted by the 1D FDM analysis, while Figures 7 and 8 show the internal temperature distributions and flow directions of the hot and cold channels predicted by the 2D FDM analysis, respectively. Similar to the design-point comparison, the 2D model under the off-design condition predicts a lower heat duty, a smaller temperature drop on the hot side, a smaller temperature rise on the cold side, and larger pressure drops compared to the 1D model. This confirms that the trends observed at the design-point are consistently maintained under off-design conditions.

Table VI: 1D and 2D FDM Analysis Results under the Off-Design Condition

	1D	2D
Hot / Cold Channel Diameter [mm]	1.8	
Length [m]	0.96	
Hot Channel Number	880000	
Cold Channel Number	880000	
Hot Inlet Temperature [℃]	640	
Hot Outlet Temperature [℃]	401.10	405.74
Cold Inlet Temperature [℃]	375	
Cold Outlet Temperature [℃]	622.76	620.32
Hot Pressure Drop [kPa]	95.16	225.85
Cold Pressure Drop [kPa]	118.77	223.83
Heat Duty [MW_{th}]	170.64	165.93

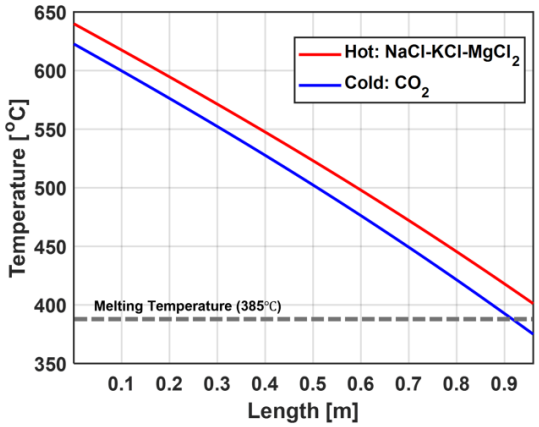

Fig. 6. IHX Temperature Distribution by 1D FDM

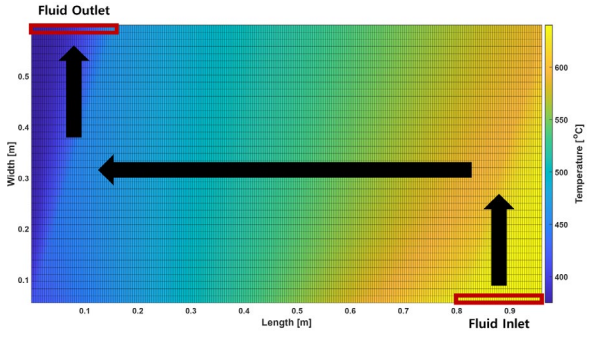

Fig. 7. IHX Hot-Side Temperature Distribution by 2D FDM

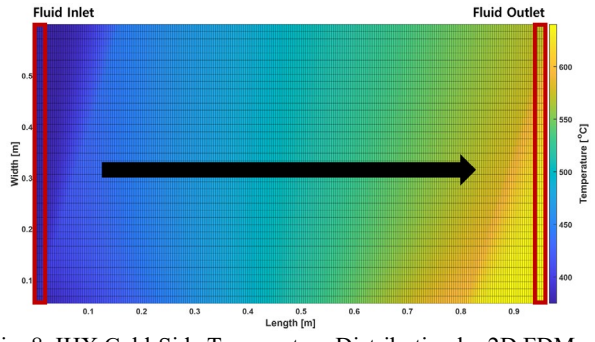

Fig. 8. IHX Cold-Side Temperature Distribution by 2D FDM

However, the most critical distinction in the off-design analysis is that the 2D model yields detailed internal temperature distributions that the 1D model cannot capture. As illustrated in Figure 7, the hot-side outlet region does not exhibit a uniform temperature. Rather, it shows a wide channel-wise temperature distribution highly dependent on the transverse position. Because the outlet temperature in the 2D analysis is calculated as the mass-flow-weighted average of the individual channel temperatures, the average outlet temperature alone fails to represent the local minimum temperature within the PCHE. In contrast, the 1D model predicts a single representative temperature profile along the streamwise direction, and thus, it cannot resolve this internal non-uniformity.

Based on this non-uniform temperature distribution, Figure 9 visualizes the localized solidification regions within the hot channel by highlighting areas where the local temperature falls below the melting point of the selected coolant-salt. These results indicate that even when the average outlet temperature remains above the melting point, specific local regions near the outlet can still reach lower temperatures depending on their channel position. This demonstrates the 2D model's capability to identify local minimum temperatures and localized solidification regions that are entirely inaccessible to the 1D model. Consequently, while the 1D model might indicate that the average outlet condition remains safely above the melting point, the 2D model reveals that localized solidification can indeed occur within the PCHE due to internal temperature non-uniformity.

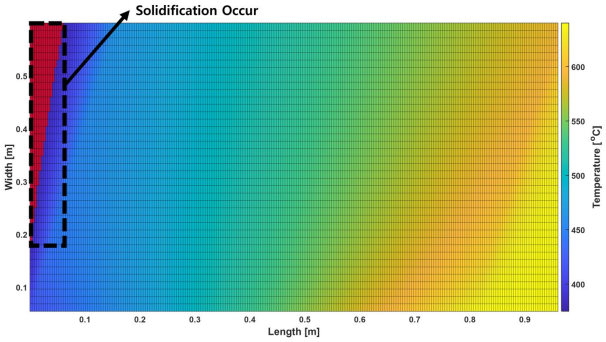

Fig. 9. Prediction of Localized Coolant-Salt Solidification Onset in the IHX by 2D FDM

It should be noted that the localized solidification regions shown in Figure 9 are identified using a conservative temperature-threshold criterion based on whether the local coolant-salt temperature falls below the melting point. In an actual phase-change process, latent heat release during solidification can buffer further local temperature reduction, and the subsequent growth of solidification may also alter the local flow and heat-transfer behavior. However, such fully coupled phase-change evolution was beyond the scope of the present study. In addition, the thermophysical-property correlations adopted in Table III were used to represent the liquid-phase behavior of the coolant-salt, and their applicability in partially or fully solidified regions was not additionally assessed in this work. Therefore, the red regions in Figure 9 should be interpreted as conservative predictions of localized solidification onset risk, rather than as direct predictions of fully developed blockage.

To further examine the possible thermal-hydraulic consequences after the onset of localized solidification, an additional 2D FDM sensitivity analysis was carried out by reducing the number of available hot-side channels to mimic partial channel blockage. For comparison, Table VII presents the baseline 2D off-design results alongside the simulated blockage results derived from that analysis.

Table VII: 2D FDM Sensitivity Analysis Results for Localized Solidification Blockage Scenarios

	Unblocked	Blocked
Hot Channel Number	880000	550000
Cold Channel Number	880000	880000
Heat Duty [MW_{th}]	165.93	168.91
Hot-Side Mass Flow Rate per Channel [kg/s]	0.00074	0.0012
Hot-Side Reynolds Number	100.31	160.46
Hot-Side Pressure Drop [kPa]	225.85	431.86
Cold-Side Pressure Drop [kPa]	223.83	230.98

When partial blockage occurs, the flow rate in the remaining open channels increases, which in turn leads to a higher Reynolds number. This phenomenon enhances the heat-transfer capability within the restricted number of channels. As a result, there is no significant difference in the overall heat transfer capability compared to the baseline condition. However, a difference arises in the pressure drop. The increased flow velocity in the remaining channels causes the hot-side pressure drop to increase to nearly twice its original value. From a system-level viewpoint, such a massive increase in pressure drop may impose an unfavorable burden on the molten-salt pumping power, even though the overall heat transfer performance remains largely unchanged.

3. Summary and Conclusions

In this study, a comparative numerical analysis based on 1D and 2D FDM was performed to investigate coolant-salt solidification behavior inside the IHX of an MSR–sCO_2 marine propulsion system. The study focused on identifying the structural limitation of the 1D FDM analysis, which simplifies the complex internal flow paths into an ideal counter-flow configuration and cannot capture the flow maldistribution near the header regions and the resulting local temperature non-uniformity. Specifically, attention was paid to the discrepancy in solidification prediction between the 1D and 2D analyses when coolant-salt is used as a hot-side working fluid with a finite melting point.

The design-point comparison first showed that under the nominal operating condition, the 2D FDM analysis

predicts lower heat duty and larger pressure drops than the 1D FDM analysis. This confirms that the discrepancy between the two models is fundamentally caused by the structural and methodological difference between the simplified ideal counter-flow assumption and the more realistic two-dimensional treatment of headers, cross-flow regions, and channel-wise flow maldistribution.

Under the off-design condition, the 1D and 2D analyses both predicted average outlet temperatures above the melting point. However, the 2D FDM analysis revealed that local temperatures in individual channels near the hot-side outlet can fall below the melting point due to the non-uniform internal temperature distribution. These localized solidification regions are captured only through the 2D FDM analysis. This clearly demonstrates that the 1D FDM model, which relies solely on average outlet temperature, cannot represent the local minimum temperature inside the PCHE and therefore underestimates the risk of localized solidification.

It should also be emphasized that the present solidification prediction is based on a conservative onset criterion using the melting point and does not explicitly include latent heat release or the subsequent evolution of solidification. Therefore, the predicted red regions in Figure 9 should be interpreted as conservative indicators of localized solidification onset risk. In addition, an additional 2D FDM sensitivity analysis with reduced hot-side channel number was carried out to mimic partial blockage after local solidification. The result showed that the overall heat duty changes only slightly, whereas the hot-side pressure drop increased significantly. This indicates that, although the overall heat-transfer rate may not deteriorate severely at the early stage of blockage, the hydraulic penalty can become much more significant from the viewpoint of system operation.

These findings suggest that although 1D FDM analysis plays a pivotal role in initial design and transient simulations due to its high computational efficiency, its structural limitations lead to an underestimation of the localized solidification risk. However, performing all system-level calculations using 2D FDM analysis is impractical due to immense computational costs. Therefore, to safely utilize the 1D model while strictly preventing solidification, more rigorous operational constraints must be applied. While applying a safety margin to the average outlet temperature might account for operational variations or uncertainties in the chemical composition of the coolant-salt, it is insufficient to completely prevent localized solidification inside the channels. To fundamentally block this risk, a strict design and control condition must be established such that the cold-side inlet temperature entering the IHX is always maintained higher than the melting point of the hot-side coolant-salt. Under this strict condition, localized solidification becomes physically impossible. Consequently, the computationally efficient 1D FDM analysis can be reliably employed without the risk of unpredicted internal solidification, providing an essential guideline for establishing design and operational strategies for future MSR–sCO_2 systems.

ACKNOWLEDGEMENT

This work was supported by the National Research Foundation of Korea(NRF) grant funded by the Korea government(MSIT) (No. RS-2025-25454059).

REFERENCES

[1] Tae-Hwan Joung, Seong-Gil Kang, Jong-Kap Lee and Junkeon Ahn, “The IMO initial strategy for reducing Greenhouse Gas(GHG) emissions, and its follow-up actions towards 2050”, *Journal of International Maritime Safety, Environmental Affairs, and Shipping*, vol. 4, pp. 1-7, 2020.

[2] Jeong Min Baek, Gihyeon Kim, Seungkyu Lee, and Jeong Ik Lee, “Assessment of Coolant-Salt Solidification Under Load-Following Operation for a Marine MSR-sCO_2 System”, Transactions of the Korean Nuclear Society Autumn Meeting, Oct.30-31, 2025, Changwon, Korea.

[3] Changye Huang, Weihua Cai, Yue Wang, Yao Liu, Qian Li, and Biao Li, “Review on the characteristics of flow and heat transfer in printed circuit heat exchangers”, *Applied Thermal Engineering*, vol. 153, pp. 190-205, 2019.

[4] Seongmin Son, Youho Lee, and Jeong Ik Lee, Development of an advanced printed circuit heat exchanger analysis code for realistic flow path configurations near header regions, International Journal of Heat and Mass Transfer, vol. 89, pp. 242-250, 2015.

[5] Carolina Villada, Wenjin Ding, Alexander Bonk, and Thomas Bauer, “Engineering molten $MgCl_2$–KCl–NaCl salt for high-temperature thermal energy storage: Review on salt properties and corrosion control strategies”, *Solar Energy Materials and Solar Cells*, vol. 232, 2021.

[6] Seungjoon Baik, Seong Gu Kim, Seong Jun Bae, Yoonhan Ahn, Jekyoung Lee, and Jeong Ik Lee, “Preliminary Experimental Study of Precooler in Supercritical CO_2 Brayton Cycle”, *Proceedings of ASME Turbo Expo 2015*, Jun, 2015, Montreal, Canada.